

Noncommutative geometry inspired charged black holes

Stefano Ansoldi

Dipartimento di Matematica ed Informatica, Università di Udine, and Istituto Nazionale di Fisica Nucleare, Sezione di Trieste, Trieste, Italy

Piero Nicolini

Dipartimento di Matematica e Informatica, Consorzio di Magnetofluidodinamica, Università degli Studi di Trieste and Istituto Nazionale di Fisica Nucleare, Sezione di Trieste, Trieste, Italy

Anais Smailagic

Istituto Nazionale di Fisica Nucleare, Sezione di Trieste, Trieste, Italy

Euro Spallucci

Dipartimento di Fisica Teorica dell' Università di Trieste, and Istituto Nazionale di Fisica Nucleare, Sezione di Trieste, Trieste, Italy

Abstract

We find a new, non-commutative geometry inspired, solution of the coupled Einstein-Maxwell field equations describing a variety of charged, self-gravitating objects, including extremal and non-extremal black holes. The metric smoothly interpolates between *deSitter* geometry, at short distance, and *Reissner-Nordström* geometry far away from the origin. Contrary to the ordinary Reissner-Nordström spacetime there is no curvature singularity in the origin neither “naked” nor shielded by horizons. We investigate both Hawking process and pair creation in this new scenario.

In a recent paper we obtained a non-commutative geometry inspired solution of the Einstein equation smoothly interpolating between a deSitter core around the origin and an ordinary Schwarzschild spacetime at large distance

¹ email: ansoldi@trieste.infn.it

² email: nicolini@cmfd.univ.trieste.it

³ email: anais@ts.infn.it

⁴ email: spallucci@trieste.infn.it

[1]. The curvature singularity at $r = 0$ is replaced by a regular deSitter vacuum accounting for the effect of non-commutative coordinate fluctuations at short distance. Furthermore, the Hawking temperature does not blow up as the event horizon shrinks down, instead it reaches a maximum value for a radius $r_H \simeq 4.7\sqrt{\theta}$ and drops down to zero at $r_H \rightarrow r_0 \simeq 3.0\sqrt{\theta}$; θ is the parameter measuring the amount of coordinate non-commutativity in the coordinate coherent states approach [2] : $[\mathbf{x}^\mu, \mathbf{x}^\nu] = i\theta\epsilon^{\mu\nu}$. Our model of “noncommutative” Schwarzschild black hole allows to answer the question: which is the endpoint of the Hawking process? This question has no definite answer neither in the framework of quantum field theory in curved spacetime, nor in string theory. In our case, we find a cold remnant given by a stable, extremal black hole, at zero temperature and radius r_0 determined by the θ parameter.

Our regular black hole has been employed as nonsingular background geometry in the study of the vacuum polarization of matter by means of the effective action approach [3]. There are other applications of the coherent state approach to gravity [4], and recently our model has been extended to large extra-dimensions scenario in [5], where it is discussed under what conditions such a kind of remnant could be produced at LHC. With this exciting perspective in mind, we think it is phenomenologically relevant ⁵ to extend our former solution to more general configurations carrying *charges* other than pure gravitational one. From this viewpoint, the immediate extension of the Schwarzschild-like objects we found in [1] amount to endow them with an “Abelian hair” in the form of an $U(1)$ electric charge and long range Coulomb-like electric field. Objects of this sort will, eventually, decay, not only through Hawking radiation, but through pair creation of charged particles [8], as well, provided the near horizon electric field is higher than the threshold critical intensity $E_{cr} = \pi m_e^2/e$. In this case, the black hole can radiate either its whole charge or a fraction of it. In the former case it reaches a Schwarzschild phase, finally approaching the degenerate, extremal configuration discussed above. In the latter case, a stable extremal Reissner-Nordström, with a residual charge, will be left out.

In this letter we are going to solve Einstein-Maxwell equations in the presence of a static, spherically symmetric, minimal width, gaussian distribution of mass and charge. The decay of the black hole type solutions will be investigated both analytically and numerically along the lines presented above.

Putting gravity aside for a moment, let us consider the effect of non-commuting coordinates on an elementary charge. We have shown that the coordinate fluctuations can be described, within coherent states approach, as a *smearing effect* [6], turning point-like mass into a “matter droplet” with a gaussian profile. As coordinate non-commutativity is a property of the spacetime fabric itself, and not of its matter content, the same smearing effect is expected to operate on electric as well as “inertial” charges, i.e. masses. Thus, a point-charge e is

⁵ *TeV* black holes decay is presently an extremely important research field in view of the experiments planned for the next generation particle colliders [7].

spread into a minimal width gaussian charge cloud according with the rule:

$$e \delta(\vec{x}) \longrightarrow \rho_{el.}(\vec{x}) = \frac{e}{(4\pi\theta)^{3/2}} \exp\left(-\vec{x}^2/4\theta\right) \quad (1)$$

For a static, spherically symmetric charge distribution, the current density J^μ is non-vanishing only along the time direction:

$$J^\mu(x) = \rho_{el.}(x) \delta_0^\mu \quad (2)$$

The system of Einstein-Maxwell field equations reads

$$R^\mu{}_\nu - \frac{1}{2} \delta^\mu{}_\nu R = 8\pi (T^\mu{}_\nu|_{\text{matt.}} + T^\mu{}_\nu|_{\text{el.}}) \quad (3)$$

$$\frac{1}{\sqrt{-g}} \partial_\mu (\sqrt{-g} F^{\mu\nu}) = J^\nu \quad (4)$$

where $T_{\text{matt.}}{}^\mu{}_\nu$ is the same as in [1], while the electromagnetic energy-momentum tensor is the usual one with $F^{\mu\nu} = \delta^{0[\mu} \delta^{r|\nu]} E(r)$.

The Coulomb-like field is obtained by solving the Maxwell equations (4) with source (2).

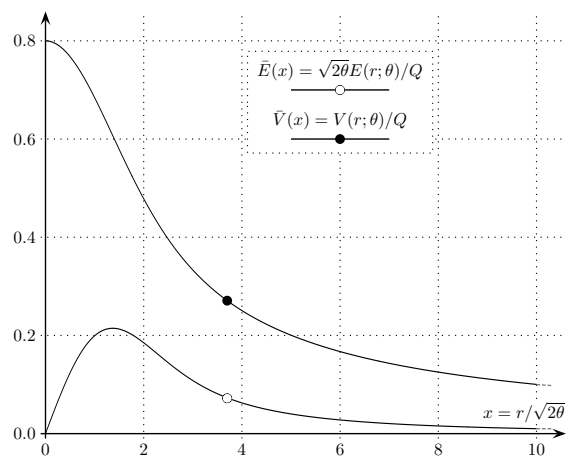


Fig. 1. *Electric field $E(r; \theta)$ (per unit charge) and corresponding Coulomb-like potential $V(r; \theta)$ (per unit charge). Smearing of the charge leads to a regular behavior at the origin. The electric field reaches its maximum intensity near $r \approx 2\sqrt{\theta}$, and then drops to zero. Long distance behavior is that of ordinary Coulomb field.*

We find the electric field to be:

$$E(r) = \frac{2Q}{\sqrt{\pi} r^2} \gamma\left(\frac{3}{2}; \frac{r^2}{4\theta}\right) \quad (5)$$

Then, solving the Einstein equations (3) we find Reissner-Nordström like the metric :

$$ds^2 = -g_{00} dt^2 + g_{00}^{-1} dr^2 + r^2 d\Omega^2 \quad (6)$$

$$g_{00} = 1 - \frac{2m(r)}{r} + \frac{Q^2}{\pi r^2} F(r) , \quad (7)$$

$$m(r) = \frac{2m_0}{\sqrt{\pi}} \gamma\left(\frac{3}{2}, r^2/4\theta\right) , \quad (8)$$

$$F(r) \equiv \gamma^2\left(\frac{1}{2}, r^2/4\theta\right) - \frac{r}{\sqrt{2\theta}} \gamma\left(\frac{1}{2}, r^2/2\theta\right) , \quad (9)$$

$$\gamma(a/b; x) \equiv \int_0^x \frac{du}{u} u^{a/b} e^{-u} \quad (10)$$

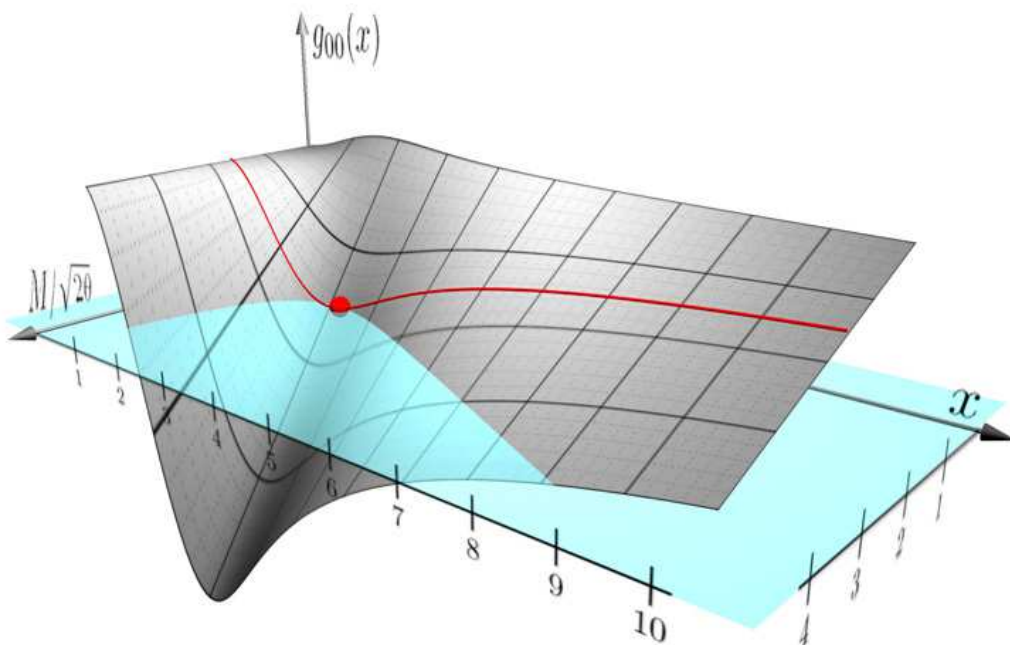


Fig. 2. g_{00} versus M and r , for a charge, $Q = 1$ in $\sqrt{\theta}$ units. The intersection of the $g_{00} = 0$ plane (cyan) with $g_{00} = g_{00}(r, M)$ surface (grey) gives the “horizon curve” whose minimum (red-dot) gives the extremal black hole. The portion of the surface below the plane $g_{00} = 0$ represents the spacelike region between inner and outer horizons.

The line element (6) shows an interesting asymptotic behavior for small r . By using the asymptotic form of the lower incomplete gamma-function one sees

that $F(r) \sim O(r^6)$ and the metric (6) is of the deSitter type

$$g_{00} = 1 - \frac{m_0}{3\sqrt{\pi}\theta^{3/2}} r^2 + O(r^4) \quad (11)$$

The vacuum energy associated to the non-commuting coordinate fluctuations shows up as an effective cosmological $\Lambda_{eff.} = m_0/\sqrt{\pi}\theta^{3/2}$ leading to a *finite curvature* in the origin: the “singularity” has been swept away by the vacuum fluctuation of the spacetime fabric itself. ⁶

It may seem surprising that there are no charge contributions to the effective cosmological constant. This is due to the linear behavior of the electric field at short distance, as seen from Fig.(1), which can only give contributions $O(r^4)$ to the metric. Thus, an observer close to the origin sees only the “bare mass” m_0 stripped from the charge dressing.

On the other hand, we want to compare our solution to the usual Reissner-Nordström geometry, at large distance. In this case, the asymptotic observer can only measure the *total mass-energy* in which he cannot distinguish anymore between gravitation and electric contribution. Thus, the total mass-energy is now define as the integrated flux of T_μ^0

$$M = \oint_{\Sigma} d\sigma^\mu \left(T_\mu^0|_{\text{matt.}} + T_\mu^0|_{\text{el.}} \right) \quad (12)$$

where, Σ , is a $t = \text{const.}$, closed three-surface.

With the definition (12) the metric (6) reads

$$g_{00} = 1 - \frac{4M}{\sqrt{\pi}r} \gamma\left(3/2, r^2/4\theta\right) + \frac{Q^2}{\pi r^2} \left[F(r) + \sqrt{\frac{2}{\theta}} r \gamma\left(3/2, r^2/4\theta\right) \right] \quad (13)$$

The asymptotic form of (13) reproduces Reissner-Nordström metric for large distances.

Depending on the values of Q and M metric displays different causal structure: existence of two horizons (non-extremal black hole), one horizon (extremal black hole) or no horizons (massive charged “droplet”), as can be seen from the plots of (13). $g_{00}(r_H) = 0$ cannot be solved analytically in r_H , in our case, but it allows to solve M in terms of r_H and Q ⁷

$$M = \frac{Q^2}{2\sqrt{2}\pi\theta} + \frac{1}{\gamma(3/2, r_H^2/4\theta)} \left[\frac{\sqrt{\pi}}{4} r_H + \frac{Q^2}{4\sqrt{\pi}r_H} F(r_H) \right] \quad (14)$$

⁶ A quite different type of regular, charged, black holes have been obtained, in the framework, of a new, non-linear, electrodynamics coupled to gravity [9].

⁷ The use of the equation relating the total mass energy of the system to the radius of the event horizon follows the approach proposed in [10], with the advantage of allowing an indepth investigation of geometry and dynamics of the system.

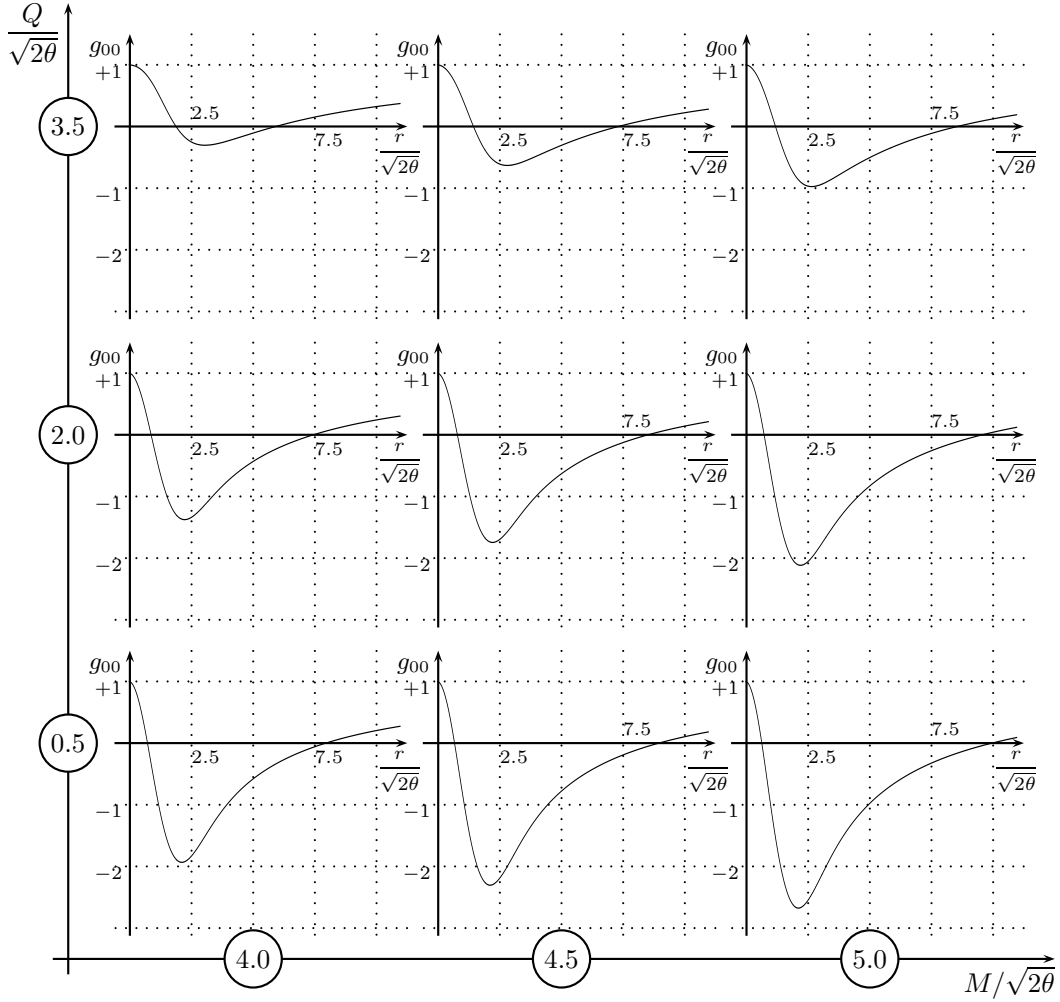


Fig. 3. g_{00} as function of r for different values of M and Q , leading to two horizons. The intersections with the r -axis gives inner and outer horizons. Given M and increasing Q $r_+ - r_- \rightarrow 0$ leading to extremal configuration. On the contrary, given Q and increasing M , enlarges the distance between horizons.

Plotting (14) is an alternative way to investigate existence and location of event horizons. To understand the information that will follow from equation (14) let us first study the simpler case of ordinary Reissner-Nordström. The corresponding function $M(r_H; Q)$ is $M = (r_H^2 + Q^2)/2r_H$.

The plot Fig.(6) consists of a family of curves labelled by the value of the electric charge Q . The horizons, and the corresponding values of M , are read as the intersections of the grid lines, with each curve in Fig.(6). It turns out that the minima of the curves define the extremal black hole configurations. All degenerate horizons lie on the dashed straight line $M = r_H$. The full straight line $M = r_H/2$ corresponds to the $Q = 0$ Schwarzschild black hole. Fig.(7) indicates that, for any given charge Q , the total mass energy of the system is

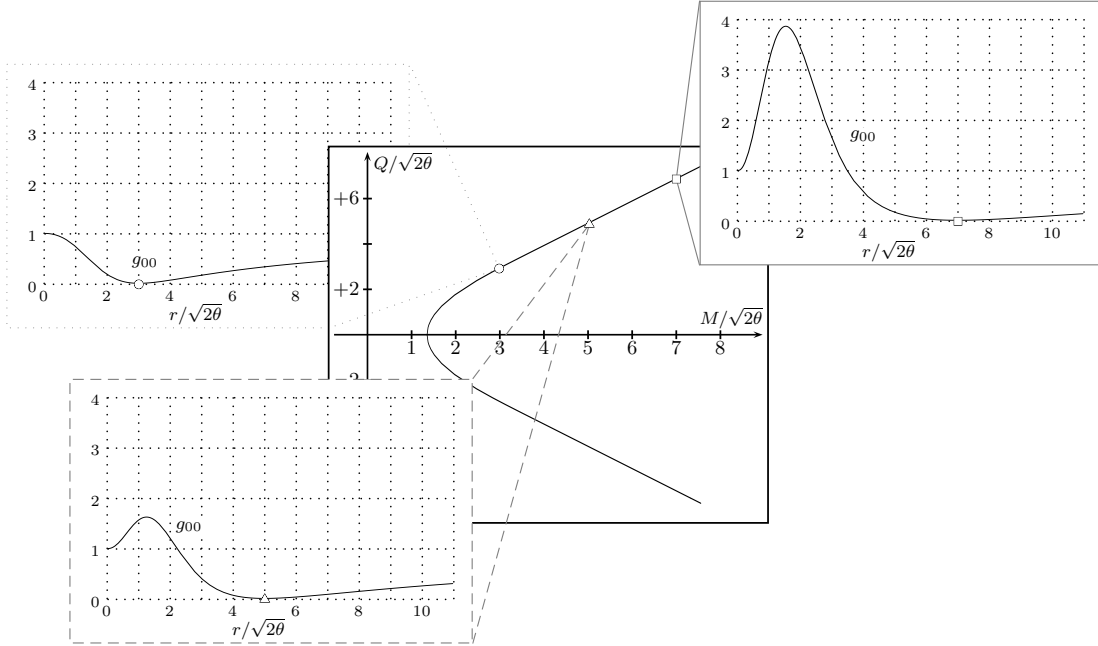


Fig. 4. g_{00} as a function of r , for M and Q leading to a single, degenerate, horizon. Extremal horizons lie on the curve in the Q, M -plane (central plot)

minimized by the extremal black hole configuration.

Thus, we conclude that every Reissner-Nordström black hole has natural tendency to evolve towards its extremal configuration.

The same kind of analysis can now be performed in the non-commutative case. In spite of complicated looking functions, e.g. $M = M(R_H; Q)$, we reach essentially same conclusions as discussed above. For this purpose we plotted (14) in Fig.(7). Once again we see that the *extremal curve* connects the minima of Q -curves, and asymptotically approaches the line $M = r_H$, in agreement with the behavior of the metric (6) at large distance. The difference between Fig.(6) and Fig.(7) is seen at short distance where we find a non-vanishing *minimal mass*, for $Q = 0$, corresponding to the extremal Schwarzschild-like black hole found in [1]. This effect is due to the non-commutativity of space-time coordinates.

Fig.(7) suggests the following scenario of the dynamical evolution of noncommutative inspired Reissner-Nordström like black holes. At the very beginning system is described by Q and r_+ , then it starts evolving towards its ground state, i.e. tends to minimize its total mass-energy. It can do it in two different ways: i) it can radiate away its mass mainly in form of neutral particles (Hawking evaporation), “sliding down” the Q -curve ; ii) it can reduce both its mass and charge through pair creation, jumping from higher to lower Q -curves. In the former case the final configuration would be an extremal Reissner-Nordström-like black hole with a residual charge, while in the latter it ends up as an extremal Schwarzschild black hole. Which evolution path will

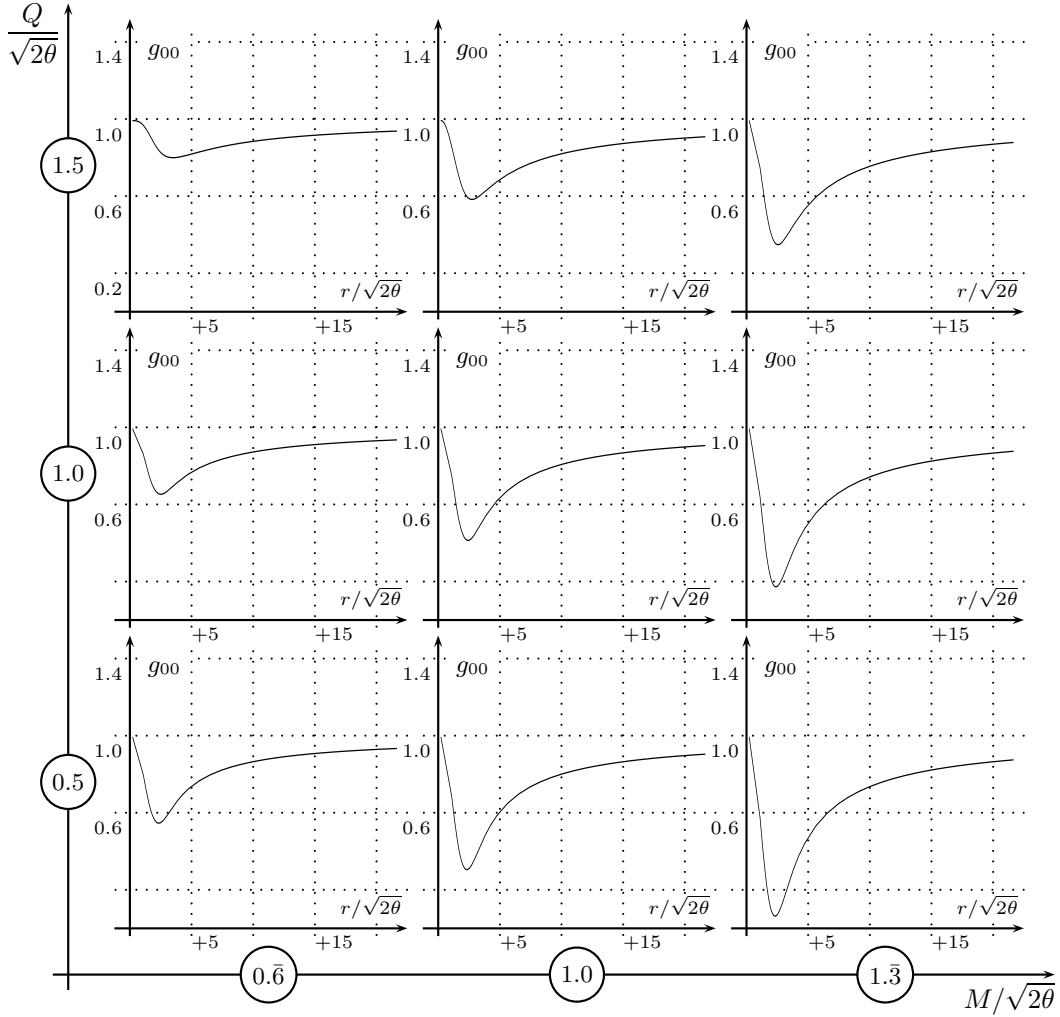


Fig. 5. g_{00} as a function of r , for values of M and Q leading to no horizons.

be taken, essentially depends on the interplay between two decay channels. In connection with the above picture, it is important to investigate the behavior of the Hawking temperature T_H . The temperature T_H is given by:

$$\begin{aligned}
4\pi T_H = & \frac{1}{r_+} \left[1 - \frac{r_+^3 \exp(-r_+^2/4\theta)}{4\theta^{3/2} \gamma(3/2, r_+^2/4\theta)} \right] + \\
& - \frac{4Q^2}{\pi r_+^3} \left[\gamma^2(3/2, r_+^2/4\theta) + \frac{r_+^3 \exp(-r_+^2/4\theta)}{16\theta^{3/2} \gamma(3/2, r_+^2/4\theta)} F(r_+) \right] \quad (15)
\end{aligned}$$

We plot T_H in Fig.(8). From Fig.(8) and Fig.(7) one infers that, instead of growing indefinitely temperature reaches a maximum value and then drops to zero at the extremal black hole configuration. This is the same behavior already encountered in the noncommutative neutral case [1]. The effect of charge is just to lower the maximum temperature.

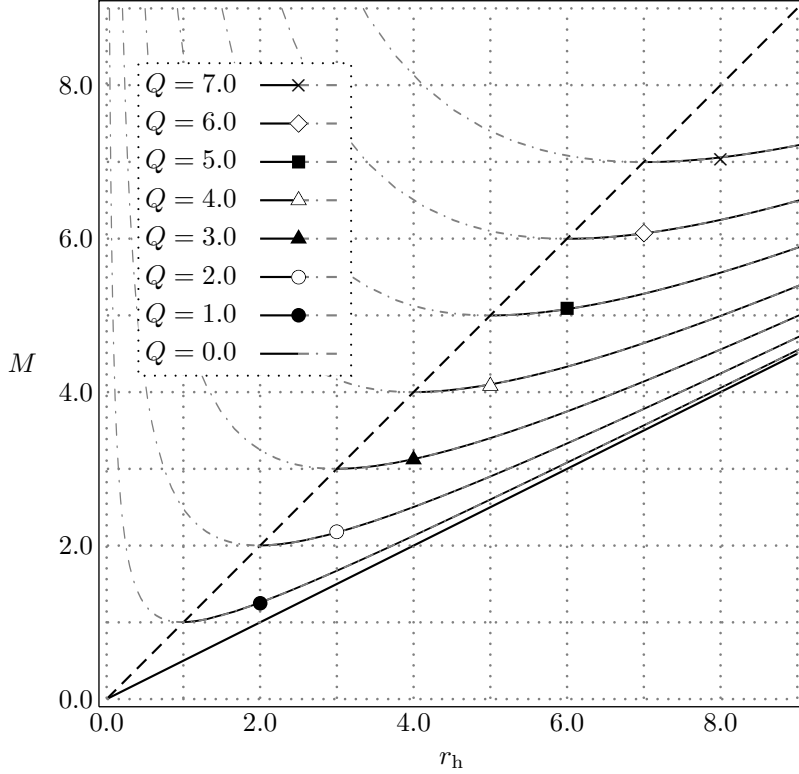


Fig. 6. M as a function of r_H for different Q in case of Reissner-Nordström black hole. The straight line $M = r_H/2$ gives the Schwarzschild black-hole. The dashed straight line $M = r_H$ intersects the minima of Q -curves representing extremal Reissner-Nordström black holes.

At this point we would like to discuss, at least qualitatively, which of the possible decay channels is more likely.

The creation of e^\pm pairs near the event horizon is described by the Schwinger formula [11]. This formula implies that in order for creation process to take place, the electric field has to exceed the *critical intensity* $E_{cr.} = \pi m_e^2/e$. In our case this condition leads to

$$\frac{2Q}{\sqrt{\pi} r_+^2} \gamma \left(\frac{3}{2}; \frac{r_+^2}{4\theta} \right) \geq \pi \frac{m_e^2}{e} \quad (16)$$

From Fig.[1] one sees that the electric field attains maximal intensity near $r \approx 2\sqrt{\theta}$, for any Q : $E_{max.} = E(r_{max.}) \approx 0.28 Q \sqrt{2\theta}$.

Let us express the total charge Q as an integer multiple of the fundamental charge e , i.e. $Q = ze$. Equation (16), with any possible value for r_+ , implies that there is creation for any $z \geq 1$ because $z \propto m_e^2 \theta \ll 1$.

Thus, we conclude that the electric field at the horizon is *always strong enough*

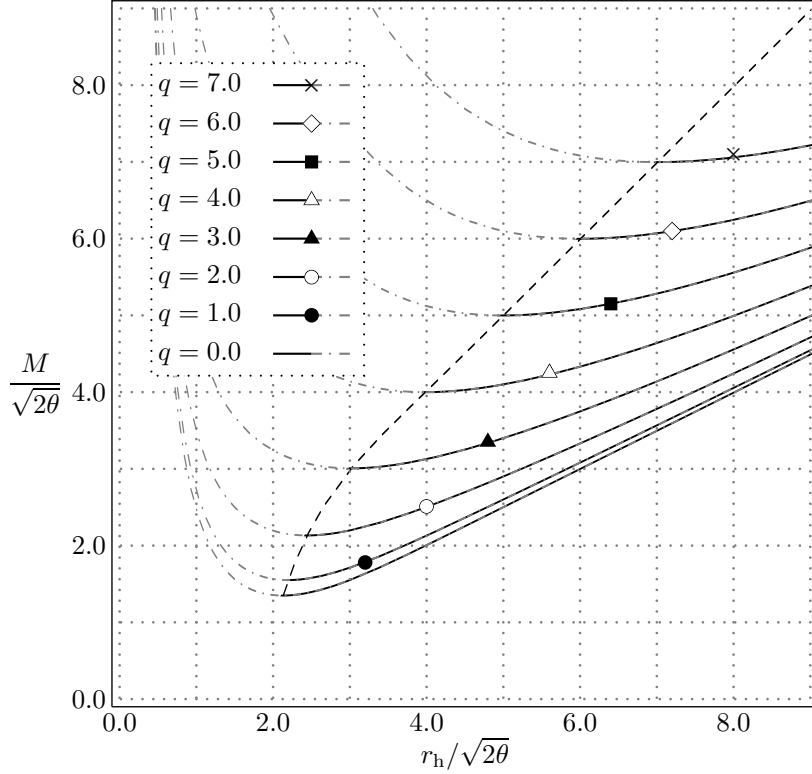


Fig. 7. M as a function of r_H for different Q in case of noncommutative Reissner-Nordström black hole. The Schwarzschild black-hole is given by the lowest curve, $Q = 0$, which is no more a straight line indicating that there can be two horizons for $M > 1.9\sqrt{\theta}$. Also in this case the dashed curve intersects the minima of Q -curves representing extremal black holes.

to create pairs. In fact, over-criticality could be attained even far away from r_+ . To verify this possibility we use the concept of *dyadosphere* introduced in [12]. Dyadosphere represents the spherical region, of radius r_{ds} , where E is strong enough to produce pairs. In our case the radius r_{ds} is determined by

$$\frac{r_{ds}^2}{\gamma\left(\frac{3}{2}; \frac{r_{ds}^2}{4\theta}\right)} = \frac{2ze^2}{\pi^{3/2}m_e^2} r_{ds}^2 \simeq \frac{2ze^2}{\pi^{3/2}m_e^2} \gamma\left(\frac{3}{2}; \frac{ze^2}{4\pi\theta m_e^2}\right) \quad (17)$$

As a first approximation we find

$$r_{ds}^2 \simeq \frac{2ze^2}{\pi^{3/2}m_e^2} \gamma\left(\frac{3}{2}; \frac{ze^2}{4\pi\theta m_e^2}\right) \quad (18)$$

Equation (18) show that the characteristic length scale of the dyadosphere is the electron Compton wavelength, which is orders of magnitude larger than

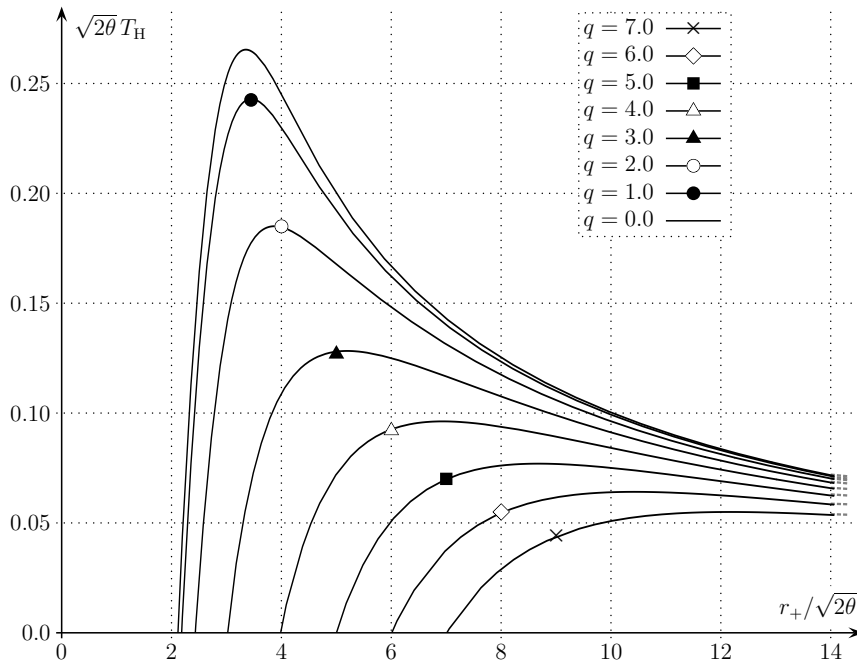


Fig. 8. Hawking temperature as a function of r_H , for different values of Q . The temperature drops to zero even in the case $Q = 0$ as a result of coordinate uncertainty. The peak temperature drops with increasing Q .

$\sqrt{\theta}$. Thus, we conclude that, for charged black holes, described by the line element (9), $r_{ds} \gg r_+$. As a consequence, these black holes are extremely unstable under pair creation. This analysis implies that Schwinger mechanism should dominate the early phase of black hole decay. Hawking radiation follows Schwinger phase. At the end, one is left with a neutral massive degenerate remnant found in [1].

In this letter we have investigated the existence of charged black holes inspired by non-commutativity of the space time manifold at short distance. We have found a Reissner-Nordström like metric. It reproduces exactly ordinary Reissner-Nordström solution at large distance, while at short distance it gives deSitter spacetime in place of a curvature singularity. Furthermore we have investigated the fate of such black hole against quantum decay. We came to the conclusion, that among possible decay channels, Schwinger pair production dominates the early stage while Hawking radiation determines the final stage. Recently, it has been proposed that our black holes could be produced at LHC [5]. This exciting phenomenological perspective could provide an experimental verification of our models.

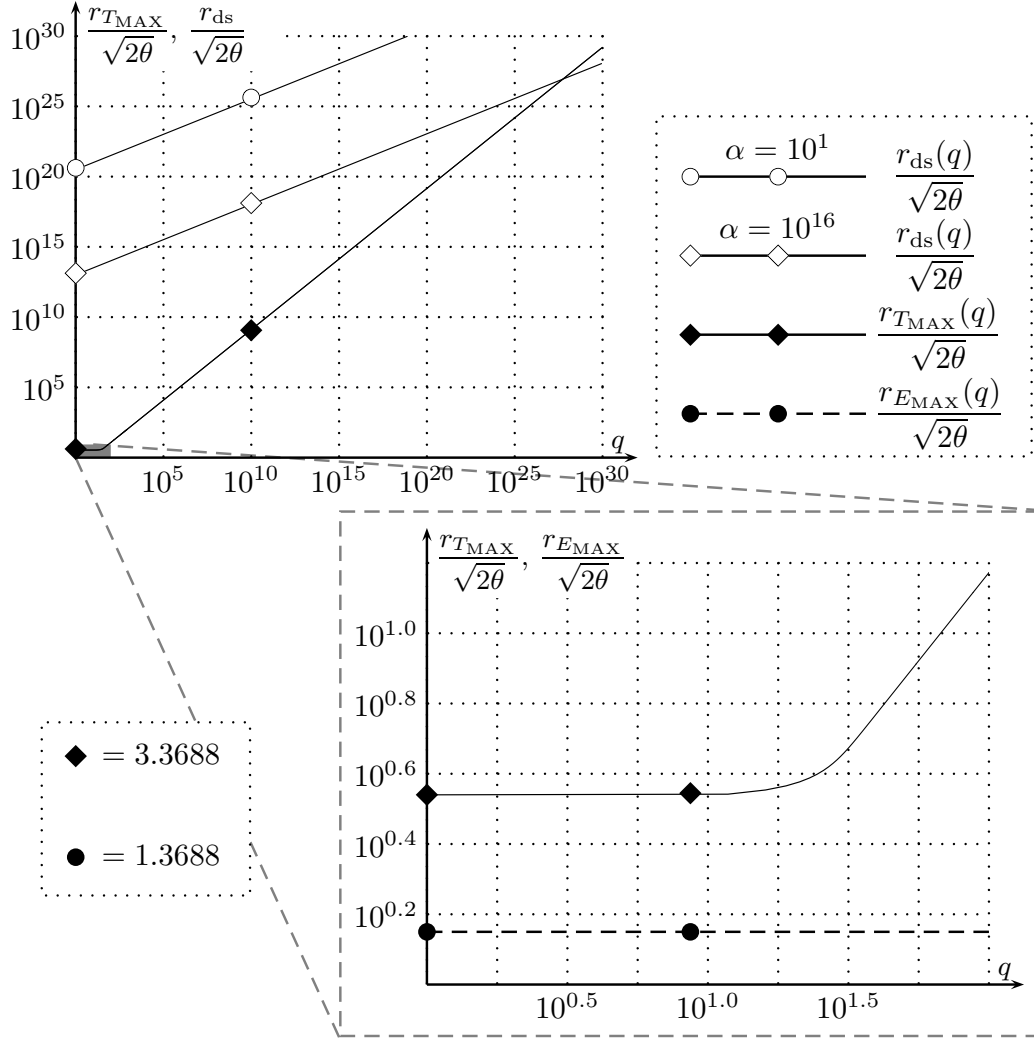


Fig. 9. Plot of the dimensionless radius at which the temperature of the black hole attains its maximum value, $r_{T_{MAX}}/\sqrt{2\theta}$, as a function of the dimensionless charge $q = Q/\sqrt{2\theta}$. All diagrams are in a bi-logarithmic scale; moreover the dimensionless charge q is expressed as a multiple of the elementary charge (for instance, on the q axis, the value 0 corresponds to the electron charge, the value 10^2 to the charge of 100 electrons, and so on). In the top diagram the dimensionless radius of the dyadosphere $r_{ds}/\sqrt{2\theta}$ is also plotted for comparison (the ratio between the non commutativity scale, $\sqrt{2\theta}$, and the Planck length, l_P , is called α , i.e. $\sqrt{2\theta} = \alpha l_P$). We see that for a wide range of charges and for values of α between 10 and 10^{16} , $r_{ds}/\sqrt{2\theta}$ largely exceeds $r_{T_{MAX}}/\sqrt{2\theta}$. In the bottom diagram the details of the above plot for a number of elementary charges between 1 and 10^2 is shown. In this case, we also plot the dimensionless radius $r_{E_{MAX}}/\sqrt{2\theta}$ at which the electric field reaches its maximum value (dashed line): this shows that always $r_{E_{MAX}}/\sqrt{2\theta} < r_{T_{MAX}}/\sqrt{2\theta}$ and also that $r_{E_{MAX}}/\sqrt{2\theta} < r_{ds}/\sqrt{2\theta}$.

Acknowledgements

We would like to thank Dr. Thomas G. Rizzo for useful discussions about the subject of this paper.

References

- [1] P. Nicolini, A. Smailagic, E. Spallucci Phys. Lett. **B632**, 547, (2006).
- [2] A. Smailagic, E. Spallucci, J. Phys. **A37**, 7169 (2004).
- [3] E. Spallucci, A. Smailagic and P. Nicolini, Phys. Rev. D **73**, 084004 (2006).
- [4] A. Gruppuso, J. Phys. A **38**, 2039 (2005);
P. Nicolini, J. Phys. A **38**, L631 (2005).
R. Casadio, P. H. Cox, B. Harms and O. Micu, Phys. Rev. D **73**, 044019 (2006).
- [5] T. G. Rizzo, “*Noncommutative Inspired Black Holes in Extra Dimensions*”, hep-ph/0606051.
- [6] A. Smailagic, E. Spallucci, J. Phys. **A36** L467 (2003);
A. Smailagic, E. Spallucci, J. Phys. **A36** L517 (2003).
- [7] S. B. Giddings, “*Black hole production in TeV scale gravity, and the future of high-energy physics*,” eConf**C010630** P328 (2001);
M. Bleicher, S. Hofmann, S. Hossenfelder, H. Stoecker Phys. Lett. **B548** 73 (2002);
M. Stenmark, Chin. J. Phys. **40** 512, (2002);
M. Cavaglia, Int. J. Mod. Phys. **A18** 1843, (2003);
A. Chamblin, F. Cooper, G. C. Nayak, Phys. Rev. **D69** 065010 (2004);
M. Cavaglia, S. Das, Class. Quant. Grav. **21** 4511 (2004);
T. G. Rizzo, JHEP **0506** 079 (2005);
T. G. Rizzo, Class. Quant. Grav. **23** 4263 (2006);
T. G. Rizzo, “*TeV-scale black holes in warped higher-curvature gravity*,” hep-ph/0510420;
A. Casanova, E. Spallucci, Class. Quant. Grav. **23** R45 (2006);
G. L. Alberghi, R. Casadio, D. Galli, D. Gregori, A. Tronconi and V. Vagnoni, “*Probing quantum gravity effects in black holes at LHC*,” hep-ph/0601243;
R. Casadio and B. Harms, Int. J. Mod. Phys. A **17**, 4635 (2002);
H. Stoecker, “*Mini black holes in the first year of the LHC*” hep-ph/0607165.
- [8] G.W. Gibbons Commun. Math. Phys. **44** 245 (1975);
T. Damour, R. Ruffini Phys. Rev. Lett. **35** 463 (1975);
T. Damour, R. Ruffini Phys. Rev. **D14** 332 (1976);
D. Garfinkle, S. B. Giddings, A. Strominger Phys. Rev. **D49** 958 (1994).
- [9] E. Ayón-Beato, A. Garca Phys. Rev. Lett. **80** 5056 (1998);

- [10] A. Aurilia, G. Denardo, F. Legovini, E. Spallucci Phys. Lett. **B147** 258 (1984);
A. Aurilia, G. Denardo, F. Legovini, E. Spallucci Nucl. Phys. B **252** 523 (1985);
A. Aurilia , R.S. Kissack, R. Mann Phys. Rev. **D35** 2961 (1987);
S. K. Blau, E. I. Guendelman , Alan H. Guth Phys. Rev. **D35** 1747, (1987);
E. Farhi, Alan H. Guth, J. Guven Nucl. Phys. **B339** 417, (1990);
- [11] G. V. Dunne, “*Heisenberg-Euler Effective Lagrangians : Basics and Extensions*”, hep-th/0406216, and references therein.
- [12] G. Preparata, Remo Ruffini, She-Sheng Xue Astron. Astrophys. **338** L87 (1998);
R. Ruffini, “*On the dyadosphere of black holes*”, astro-ph/9811232.